Lipid Polymorphism Induced by Surfactant Peptide SP-B_{1-25}

R. Suzanne Farver,[†‡] Frank D. Mills,[†‡] Vijay C. Antharam,[†‡] Janetricks N. Chebukati,[§] Gail E. Fanucci,[§] and Joanna R. Long[†‡*]

[†]Department of Biochemistry and Molecular Biology, [‡]McKnight Brain Institute, and [§]Department of Chemistry, University of Florida, Gainesville, Florida

ABSTRACT Pulmonary surfactant protein B (SP-B) is an essential protein for lowering surface tension in the alveoli. SP-B_{1-25}, a peptide comprised of the N-terminal 25 amino-acid residues of SP-B, is known to retain much of the biological activity of SP-B. Circular dichroism has shown that when SP-B_{1-25} interacts with negatively charged lipid vesicles, it contains significant helical structure for the lipid compositions and peptide/lipid ratios studied here. The effect of SP-B_{1-25} on lipid organization and polymorphisms was investigated via DSC, dynamic light scattering, transmission electron microscopy, and solid-state NMR spectroscopy. At 1-3 mol% peptide and physiologic temperature, SP-B_{1-25} partitions at the interface of negatively charged PC/PG lipid bilayers. In lipid mixtures containing 1-5 mol% peptide, the structure of SP-B_{1-25} remains constant, but ^{2}H and ^{31}P NMR spectra show the presence of an isotropic lipid phase in exchange with the lamellar phase below the T_m of the lipids. This behavior is observed for both DPPC/POPG and POPC/POPG lipid mixtures as well as for both the PC and PG components of the mixtures. For 1-3 mol% SP-B_{1-25}, a return to a single lamellar phase above the lipid mixture T_m is observed, but for 5 mol% SP-B_{1-25} a significant isotropic component is observed at physiologic temperatures for DPPC and exchange broadening is observed in ^{2}H and ^{31}P NMR spectra of the other lipid components in the two mixtures. DLS and TEM rule out the formation of micellar structures and suggest that SP-B_{1-25} promotes the formation of a fluid isotropic phase. The ability of SP-B_{1-25} to fuse lipid lamellae via this mechanism, particularly those enriched in DPPC, suggests a specific role for the highly conserved N-terminus of SP-B in the packing of lipid lamellae into surfactant lamellar bodies or in stabilizing multilayer structures at the air-liquid interface. Importantly, this behavior has not been seen for the other SP-B fragments of SP-B_{8-25} and SP-B_{59-80}, indicating a critical role for the proline rich first seven amino acids in this protein.

INTRODUCTION

Pulmonary surfactant (PS) is a lipid-rich substance containing key proteins that minimizes surface tension in the alveoli. PS is required for normal respiration and provides a barrier against disease (1–3). PS is synthesized, processed into lamellar bodies, secreted, and recycled by type II epithelial cells, which cover ~5% of the alveolar gas exchange surface. PS lipids undergo a cycle of adsorption and resorption from the fluid subphase to maintain a surface-active layer at the alveolar air-fluid interface, with lung surfactant being completely recycled every 5–10 h (4).

Mammalian PS has a highly conserved lipid composition dominated by zwitterionic PCs (70–80%) and anionic PG and PI (10–20%) (5,6). Approximately 50% of the PC lipids and almost all of the anionic lipids in lung surfactant are monounsaturated. However, a significant fraction of PS (>40% of the lipids) is fully saturated DPPC, and this component is conserved among mammalian species. DPPC enhances the stability of lipid monolayers at air-water interfaces, which is of particular relevance to lung function. However, the lipid composition of PS alone is not sufficient to maintain the organization and dynamics of the lipid assemblies observed in the lung surfactant fluid of intact lung tissue. It has been postulated that protein-induced lipid polymorphisms and protein-induced trafficking of lipids to the interface are critical for PS function at ambient pressure (7–10). To support this claim, it has been shown that surfactant proteins B and C (SP-B and SP-C, respectively), which are highly hydrophobic and present at relatively low levels, are essential for imparting the recycling properties of LS. In particular, surfactant protein B (SP-B), which accounts for 0.7–1.0% of the dry weight of PS or <0.2 mol% relative to the lipids, is required for proper lung function (11,12). Inadequate PS is a leading cause of respiratory distress syndrome in premature infants (13).

The native form of SP-B is a highly hydrophobic, 17 kDa sulfhydryl-linked homodimer (14). Intramolecular disulfide bridges formed by the remaining six cysteine residues and a sequence similar to sphingolipid-activator proteins place SP-B in the saposin-like protein family. However, SP-B is significantly more lipophilic than other saposin-like proteins, and has not been found to activate lipids for enzymatic modification. The hydrophobicity and disulfide

Submitted April 28, 2010, and accepted for publication June 28, 2010.

*Correspondence: jrlong@mbi.ufl.edu

Abbreviations: CD, circular dichroism; DLS, dynamic light scattering; DPPC, 1,2-dipalmitoyl-*sn*-glycero-3-phosphocholine; DPPC-d_{62}, 1,2-d_{62}-dipalmitoyl-*sn*-glycero-3-phosphocholine; DSC, differential scanning calorimetry; EM, electron microscopy; FTIR, Fourier transform infrared; LUV, large unilamellar vesicle; MLV, multilamellar vesicle; P/L, peptide/lipid molar ratio; PC, phosphatidylcholine; PG, phosphatidylglycerol; PI, phosphatidylinositol; POPC, 1-palmitoyl-2-oleoyl-*sn*-glycero-3-phosphatidylcholine; POPC-d_{31}, 1-d_{31}-palmitoyl-2-oleoyl-*sn*-glycero-3-phosphatidylcholine; POPG, 1-palmitoyl-2-oleoyl-*sn*-glycero-3-phosphatidylglycerol; POPG-d_{31}, 1-d_{31}-palmitoyl-2-oleoyl-*sn*-glycero-3-phosphatidylglycerol; SP-B, surfactant protein B; TEM, transmission electron microscopy.

Editor: David D. Thomas.

0006-3495/10/09/1773/10 $2.00

doi: 10.1016/j.bpj.2010.06.076

bridges within SP-B make it difficult to express and purify heterologously. Animal sources of lung surfactant are the current standard of care therapeutically, posing a risk of infection or immune response (15).

Given the tremendous importance of SP-B for surfactant function, surfactant replacement methods employing simple peptide analogs with surface-active properties have been the focus of many investigations. N- and C-terminal peptide fragments of SP-B, 20–25 amino acids in length, possess significant surface activity and can restore lung compliance in mouse models of respiratory distress (16–19). Additionally, a simple peptide analog (known as KL_4) based on the hydrophilic and hydrophobic periodicity in the C-terminus has shown clinical success (20), and peptoid analogs are also surface-active (21). The N-terminal 25-residue peptide, SP-$B_{1\text{-}25}$, has been shown to not only improve the surface activity of lipid mixtures, but also to be more resistant to inhibition by the plasma protein fibrinogen compared to the full protein (22). More recently, a chimeric construct made up of the C- and N-terminal sequences (termed mini-B) has shown increased activity relative to the individual peptides and is comparable in activity to native SP-B at similar concentrations (23). The success of this synthetic analog suggests that both the N- and C-terminal sequences in SP-B are important for its function and may have complementary roles.

We recently reported that at therapeutically relevant concentrations, both SP-$B_{59\text{-}80}$ and KL_4 differentially partition into lipid bilayers of varying saturation while preserving a lamellar phase (24,25). The helical secondary structures of both SP-$B_{59\text{-}80}$ and KL_4 in a lipid bilayer environment vary from canonical α-helices, and both undergo changes in helicity with varying lipid composition, suggesting that structural plasticity is important to their mechanism of action. SP-$B_{1\text{-}25}$ has also been shown to possess significant helical structure when it is associated with lipid monolayers and bilayers (26–28). On the basis of FTIR and CD measurements, it has been inferred that the proline-rich N-terminal residues of SP-$B_{1\text{-}25}$ are not highly structured. Monolayer studies have demonstrated these residues are important to its rapid insertion into lipid films (19).

The effect that SP-$B_{1\text{-}25}$ has on lipid organization and polymorphisms has not been thoroughly investigated. The ability of SP-$B_{1\text{-}25}$ to modulate the macroscopic organization of lipid molecules may play a functional role in maintaining reservoirs of LS lamellar bodies near the air-water interface (10). Here we report that SP-$B_{1\text{-}25}$ can induce nonlamellar lipid morphologies when mixed with PS lipids. We utilized static ^2H and ^{31}P NMR, CD, DLS, TEM, and DSC to characterize 4:1 DPPC/POPG and 3:1 POPC/POPG lipid mixtures upon addition of varying concentrations of SP-$B_{1\text{-}25}$. The former lipid composition was selected to mirror the lipid composition of several model PS studies and lucinactant, a synthetic formulation under development for treating respiratory distress syndrome, whereas the latter composition is similar to formulations used in numerous studies of amphipathic membrane-active peptides (29) and allows for a direct comparison of the physical properties of SP-$B_{1\text{-}25}$ to SP-$B_{59\text{-}80}$ and KL_4. Lipid phases enriched in either POPC/POPG or DPPC/POPG could potentially be found in localized areas of the alveoli during the surfactant cycle.

MATERIALS AND METHODS

Synthesis of SP-$B_{1\text{-}25}$ and preparation of peptide/lipid samples

SP-$B_{1\text{-}25}$ (FPIPLPYCWLCRALIKRIQAMIPKG) was synthesized via solid-phase peptide synthesis, purified by reverse-phase high-performance liquid chromatography, and verified by mass spectrometry (m/z = 2928). Peptide was dissolved in methanol and analyzed by amino acid analysis for concentration (Molecular Structure Facility, University of California, Davis). POPC, DPPC, POPG, POPC-d_{31}, DPPC-d_{62}, and POPG-d_{31} chloroform solutions (Avanti Polar Lipids, Alabaster, AL) were quantified by phosphate analysis (Bioassay Systems, Hayward, CA). SP-$B_{1\text{-}25}$ in methanol was added to the lipid chloroform solutions resulting in P/L ratios ranging from <1:1000 to 1:20. Samples were dried under nitrogen at >45°C, suspended in warm cyclohexane (>45°C), flash frozen in nitrogen, and lyophilized to remove residual solvent.

CD experiments

CD spectra were acquired at 45°C on an Aviv Model 215 (Lakewood, NJ). Samples were prepared by hydrating lyophilized peptide-lipid powders in 10 mM HEPES buffer, pH 7.4, with 140 mM NaCl and 1 mM EDTA, to achieve a final concentration of 36 μM SP-$B_{1\text{-}25}$. Samples were extruded through 100 nm filters (Avanti Polar Lipids) to form LUVs. Spectra of 40 μM SP-$B_{1\text{-}25}$ in methanol were also collected.

DSC analysis

Thermograms were collected on a VP-DSC microcalorimeter (Microcal, Northampton, MA). Samples were prepared by solubilizing peptide-lipid powders as above to achieve a 2.5 mM lipid concentration. The samples were extruded and degassed.

Solid-state NMR analysis

^{31}P and ^2H NMR data were collected on a 500 MHz Bruker DRX system (Billerica, MA) with a 5 mm BBO probe. For the ^{31}P NMR experiments, 25 kHz proton decoupling was employed. ^2H NMR spectra were collected using a quad echo sequence (90°-τ-90°-τ-acq with τ = 30 μs). For each NMR sample, ~20 mg of peptide-lipid powder were placed in a 5 mm diameter NMR tube and 200 μL of buffer containing 10 mM HEPES, pH 7.4, 140 mM NaCl, and 1 mM EDTA in ^2H depleted water (Cambridge Isotopes, Andover, MA) were added. The hydrated dispersions were subjected to five freeze-thaw cycles to form MLVs. DePaking of NMR data was accomplished with previously published algorithms that simultaneously dePake and determine macroscopic ordering in partially aligned lipid spectra using Tikonov regularization (30). Assignments of ^2H resonances were made based on Petrache et al. (31).

DLS measurements

DLS measurements were performed using a Brookhaven 90Plus/BI-MAS ZetaPALS spectrometer with BI-9000AT Digital Autocorrelator and

9KDLSW data acquisition software. The instrument was operated at a wavelength of 659 nm over a temperature range of 25–45°C. The samples contained a 1 mM suspension of 4:1 DPPC/POPG MLVs.

TEM analysis

TEM images of 4:1 DPPC/POPG MLVs were captured using a Hitachi H-7000 transmission electron microscope operated at 75 kV with a Soft-Imaging System MegaViewIII and AnalySIS digital camera (Lakewood, CO). Samples were prepared as above and contained a 1 mM suspension of 4:1 DPPC/POPG MLVs. Sample grids were prepared by negative staining.

RESULTS

SP-B_{1-25} adopts a stable, primarily helical structure in the presence of lipid vesicles

CD spectroscopy was utilized to investigate the conformation of SP-B_{1-25} in the presence of 4:1 DPPC/POPG and 3:1 POPC/POPG unilamellar lipid vesicles (Fig. 1 *A*). The CD spectra at 45°C are identical for the two lipid environments and have features characteristic of helical secondary structure, with minima at 208 and 222 nm. Standard deconvolution analysis (32) gives secondary structure estimates of 60% α-helix, 30–35% random coil, and <10% β-sheet for SP-B_{1-25} interacting with phospholipid LUVs. These findings are consistent with results from previous FTIR studies of isotopically enriched SP-B_{1-25} in POPG, which concluded that the peptide forms a well-structured α-helix from residues 8–22 and a β-sheet conformation in the first six residues (27). The CD spectra for the peptide in the lipid-containing samples are identical for both lipid mixtures and over a concentration range of 1–5 mol% SP-B_{1-25}. A CD spectrum obtained for SP-B_{1-25} in methanol (*dashed line*), where the peptide is more helical, is also shown for comparison.

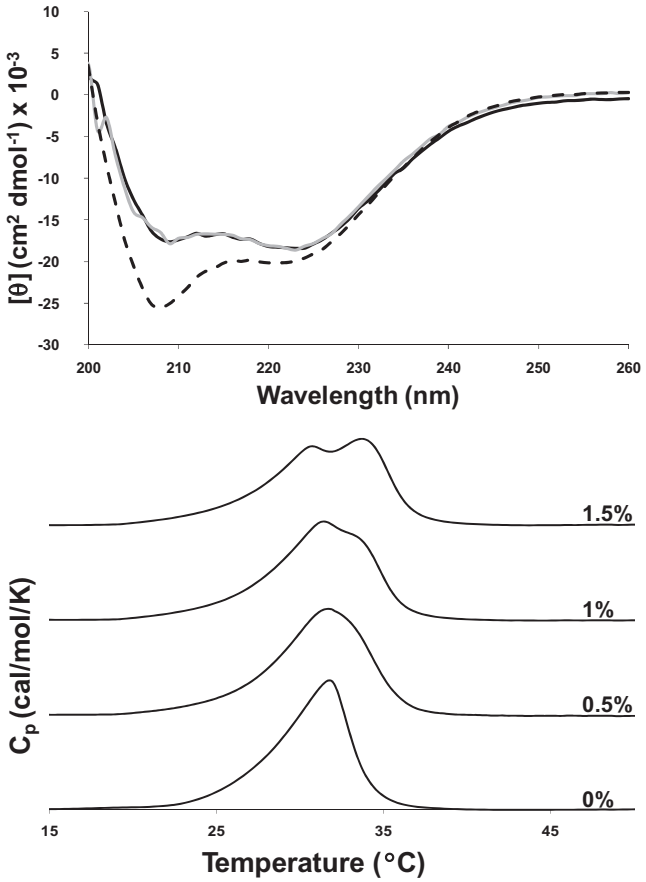

FIGURE 1 (*Top*) CD spectra at 45°C of SP-B_{1-25} at a P/L molar ratio of 1:100, 1:33, and 1:20 averaged together in 4:1 DPPC/POPG (*black solid line*) and in 3:1 POPC/POPG (*gray solid line*). The CD lineshapes for the individual P/L molar ratios are identical. A spectrum of SP-B_{1-25} dissolved in MeOH is shown for comparison (*dashed line*). The final peptide concentration was ~40 μM in all samples. (*Bottom*) DSC scans for 4:1 DPPC/POPG LUVs with SP-B_{1-25} at the indicated molar peptide percentages. The onset of phase separation is apparent at a P/L ratio of 1:200 and continues with increasing amounts of peptide.

DSC shows that SP-B_{1-25} decreases lipid miscibility

Shown in Fig. 1 *B* are DSC thermograms for 4:1 DPPC/POPG LUVs containing varying molar percentages of SP-B_{1-25}. Samples for DSC measurements had the same lipid compositions as those used for the NMR investigations described below, i.e., they included deuterated lipids (DPPC-d_{62}), the presence of which is known to lower the lipid phase transition temperature. The main phase transition temperature for the 4:1 DPPC/POPG sample is observed at 32°C. At 0.5 mol% SP-B_{1-25}, a higher temperature shoulder appears at ~34°C in the thermogram. The intensity of this shoulder grows as the concentration of peptide increases. At 1.5 mol% peptide, two separate melting events are resolved with T_m values of 31°C and 34°C, suggestive of lipid demixing or domain separation. This effect on the DSC thermogram is similar to that previously noted for the lung surfactant peptides KL_4 (33) and SP-B_{59-80} (24). Similar effects on the DSC thermograms for 7:3 DPPC-d_{62}/POPG and 7:3 DPPC/POPG-d_{31} with and without 3.5% SP-B_{8-25} (by weight) have been observed (34). From DSC data alone, one cannot distinguish whether the two transitions result from the formation of separate POPG-enriched and POPG-depleted DPPC lipid domains or whether the different melting temperatures arise from phase separation of bulk lipids and peptide-associated lipids (35) or a combination of the two, such as DPPC-peptide separation from DPPC-POPG domains.

^{2}H NMR spectra indicate that SP-B_{1-25} decreases PC/PG lipid miscibility and induces an isotropic phase, particularly for PC lipids

To obtain a molecular-level view of how SP-B_{1-25} modulates lipid organization and mixing, solid-state ^{2}H NMR spectra of both saturated and unsaturated lipid mixtures containing

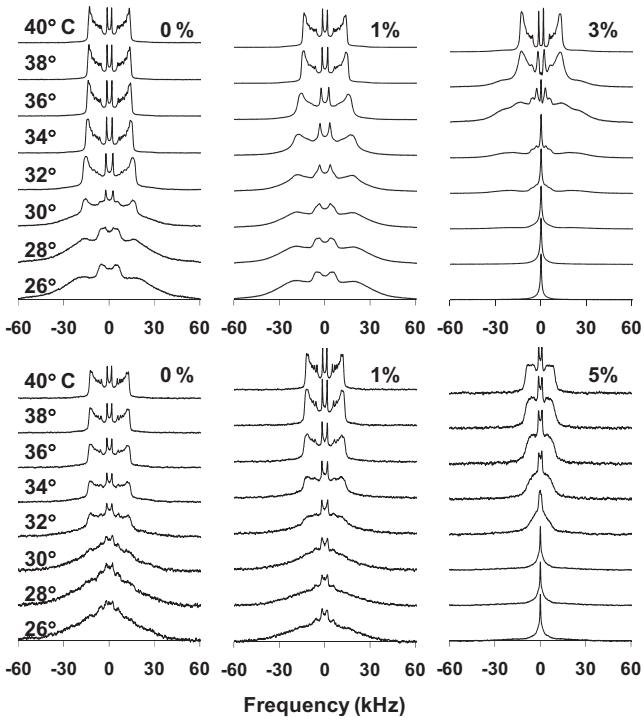

FIGURE 2 Deuterium NMR spectra as a function of temperature for (*top*) 4:1 DPPC-d_{62}/POPG MLVs and (*bottom*) DPPC/POPG-d_{31} MLVs with SP-$B_{1\text{-}25}$ added at the indicated molar percentages.

varying mol% SP-$B_{1\text{-}25}$ were obtained and analyzed. Samples containing either deuterated PC or PG were prepared, which allowed the monitoring of individual lipid components. Fig. 2 shows stack plots of ^{2}H NMR data obtained for 4:1 DPPC/DOPG samples with varying mol% SP-$B_{1\text{-}25}$ over a temperature range of 26°C to 40°C. In the absence of peptide, both the DPPC and POPG components are observed to melt at similar temperatures. The phase transition temperatures for DPPG and POPG were determined from sigmoidal fits to first-moment analyses of spectra collected between 22°C and 44°C. The phase transition temperature determined for deuterated DPPC is slightly lower (30.8°C) than that for deuterated POPG (32.8°C). This difference is likely due to a larger relative percentage of the fatty acyl chains being deuterated in the DPPC-d_{62}-containing sample compared to that of the POPG-d_{31}-containing sample (80% vs. 10%) (36). For non-peptide-containing samples, the spectra at intermediate melting temperatures, from 26 to 32°C, have lineshapes that are a superposition of gel phase and liquid crystalline phase spectra, consistent with the broad asymmetric DSC thermogram obtained for this lipid mixture. The addition of 1 mol% SP-$B_{1\text{-}25}$ increases the phase transition of the DPPC lipids, with the melting midpoint determined to be 34.3°C, whereas the melting temperature of the POPG component is not altered. These results are consistent with the DSC thermograms, where a shoulder at 34°C is detected for this concentration of SP-$B_{1\text{-}25}$, and they suggest some demixing of DPPC from the mixture on addition of SP-$B_{1\text{-}25}$. Of more interest, however, is the phase behavior seen with 3 mol% SP-$B_{1\text{-}25}$. At this peptide concentration, DPPC-d_{62} spectra from 22°C to 32°C are dominated by an isotropic peak that changes abruptly to a gel phase spectral lineshape over 34–36°C, followed by the formation of a liquid crystalline lamellar phase at 38–40°C. The lamellar phase spectrum at 38°C has significant signal intensity at the parallel edges of the lineshape relative to spectra at higher temperatures, which is consistent with more-rounded vesicles at this temperature. At higher temperatures the vesicles elongate in the magnetic field, leading to a loss of signal at the parallel edges, as is commonly seen with lipid mixtures at these high magnetic field strengths. With 5 mol% SP-$B_{1\text{-}25}$, an isotropic phase is observed for DPPC-d_{62} over the entire 26–40°C temperature range with the appearance of an anisotropic phase at 40°C. Spectra acquired up to 44°C contained a significant isotropic component (see Fig. S1 in the Supporting Material). The POPG-d_{31} spectra show less of an alteration in lipid behavior at 5 mol% peptide concentrations, but they are affected nonetheless. At 5 mol% SP-$B_{1\text{-}25}$, the spectra for POPG-d_{31} show trends very similar to those observed for DPPC-d_{62} in the presence of 3 mol% SP-$B_{1\text{-}25}$ (Fig. 2). Given these observations, it is likely that the addition of peptide causes DPPC and POPG to partially demix over the phase transition temperatures with addition of peptide, particularly at physiologic temperatures. This is in agreement with the DSC data presented above. Of interest, the cationic peptide has a larger effect on the phase behavior of the zwitterionic DPPC than the anionic POPG, as the isotropic DPPC spectra suggest that the peptide preferentially interacts with the DPPC-enriched domain.

Differences in the peptide's effects on DPPC and POPG lipid morphology in DPPC/POPG lipid mixtures may be attributed to different interactions of the peptide with the lipid headgroups, differences in partitioning due to their differing fatty acid saturation, or both. A third major lipid component of lung surfactant is POPC, which has a molecular structure intermediate between DPPC and POPG. We also investigated the effects of SP-$B_{1\text{-}25}$ on the thermotropic and phase behavior of 3:1 POPC/POPG mixtures. To compare the phase transition behavior of POPC/POPG mixtures upon addition of SP-$B_{1\text{-}25}$, we collected ^{2}H NMR data for 3:1 POPC/POPG samples containing either POPC-d_{31} or POPG-d_{31} over the temperature range of the phase transition for the monounsaturated lipids, which is ~40°C lower than the DPPC/POPG mixture (Fig. S2). A comparison of the trends for the POPC/POPG samples with the DPPC/POPG samples near the respective phase transition temperatures of the lipid mixtures indicates that these mixtures behave very similarly, with the PC lipids being more affected by the addition of SP-$B_{1\text{-}25}$ and with both systems showing the induction of an isotropic phase by the peptide. The phase transition observed for deuterated POPC is at

a slightly lower temperature (midpoint of −4.3°C) than that for deuterated POPG (−3.0°C) because a larger percentage of the lipids are deuterated in the POPC-d_{31}-containing sample (75% vs. 25%). The addition of 1 mol% SP-B_{1-25} increases the phase transition temperature of the POPC lipids by almost 6°C, with the melting midpoint at 1.2°C. In contrast, the transition temperature of the POPG lipids increases only 3.1°C, with a midpoint of 0.1°C. With 3 mol% SP-B_{1-25}, the spectra for the POPC-d_{31} lipids exhibit an isotropic peak at temperatures below the T_m of the lipids, which coalesces into a gel phase lineshape near the phase transition temperature (−2°C to 4°C), followed by the formation of a liquid crystalline lamellar phase at higher temperatures. With 5 mol% SP-B_{1-25}, an isotropic phase is observed for POPC-d_{31} over the entire low temperature range (−6°C to 4°C), with the appearance of an anisotropic lineshape beginning at 4°C. The POPG-d_{31} spectra show less of an alteration in lipid behavior at similar peptide concentrations, but they also show the appearance of an isotropic peak at lower temperatures and higher peptide concentrations. The spectra for POPG-d_{31} in a sample containing 5 mol% SP-B_{1-25} show trends very similar to those observed for POPC-d_{31} in the presence of 3 mol% SP-B_{1-25}.

From the ^{2}H NMR data it is clear that lipid headgroup composition (PC versus PG) plays a role in determining the phase behavior of the individual lipids in mixtures containing SP-B_{1-25}. The effects of the peptide on lipid morphology are also determined by the degree of saturation in the lipids. This can clearly be seen by comparing the dynamics of each of the lipids in the DPPC/POPG and POPC/POPG mixtures at the average mammalian physiologic temperature of 38°C (Fig. 3). At this temperature, the DPPC lipids are most affected by the addition of peptide and exhibit isotropic phase behavior at 5 mol% SP-B_{1-25}. Even at 3 mol% peptide the DPPC lipids are in exchange between lipid phases, as evidenced by the broadened lineshape. In contrast, the POPC and POPG lipids exhibit a lamellar lineshape even at 5 mol% peptide, although the lineshape is somewhat broadened, suggesting that an exchange between lipid phases may be occurring.

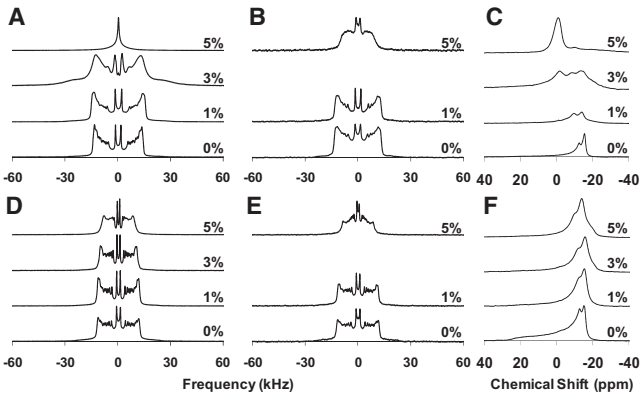

FIGURE 3 Deuterium and phosphorous NMR spectra taken at 38°C. (*A*) ^{2}H spectra of 4:1 DPPC-d_{62}/POPG MLVs, (*B*) ^{2}H spectra 4:1 DPPC/POPG-d_{31} MLVs, (*C*) ^{31}P spectra of 4:1 DPPC-d_{62}/POPG MLVs, (*D*) ^{2}H spectra of 3:1 POPC-d_{31}/POPG MLVs, (*E*) ^{2}H spectra of 3:1 POPC/POPG-d_{31} MLVs, and (*F*) ^{31}P spectra of 3:1 POPC-d_{31}/POPG MLVs with SP-B_{1-25} at the indicated molar percentages.

^{31}P NMR spectra are consistent with dynamic exchange between the isotropic and lamellar phases on a kHz timescale

At 11.7 T, phospholipid phosphorus chemical shift anisotropy tensors are more than an order of magnitude smaller than the deuterium quadrupolar coupling for a methylene group. Thus, static ^{31}P NMR spectra are more sensitive to slower motions, such as exchange between lipid phases. ^{31}P NMR spectra at 38°C for 3:1 POPC/POPG and 4:1 DPPC/POPG MLVs containing various concentrations of SP-B_{1-25} are also shown in Fig. 3. Because the data were collected on a 500 MHz NMR spectrometer, macroscopic alignment of the vesicles occurred, causing a decrease in the downfield features (parallel edges) of the lamellar lineshapes for the phospholipid dispersions. However, the perpendicular edges of the PG and PC lipid powder lineshapes (at −11 and −15 ppm, respectively) can be clearly distinguished due to slight differences in the average orientation of their respective phosphate headgroups relative to the plane of the lipids (24,25). In the DPPC/POPG mixtures, the addition of 3 mol% SP-B_{1-25} leads to the appearance of an isotropic peak concurrent with a loss of intensity at the perpendicular edge for DPPC. At 5 mol% peptide, the isotropic peak dominates the spectrum and the perpendicular edge of the POPG lineshape is also significantly less intense, consistent with exchange between a lamellar phase and an isotropic phase. In the POPC/POPG mixtures, the addition of peptide has less of an effect on the ^{31}P lineshapes at 38°C; an isotropic peak is not observed. However, there is sufficient lipid exchange to observe altered lineshapes in samples containing 3 and 5 mol% peptide. ^{31}P spectra as a function of temperature for both DPPC/POPG and POPC/POPG are provided in Fig. S3. Significant isotropic components are observed in the spectra near the phase transition temperatures of the lipid mixtures on addition of SP-B_{1-25}, consistent with the ^{2}H NMR data. The persistence of an isotropic peak in the ^{31}P spectra at temperatures where ^{2}H spectra are anisotropic (e.g., compare ^{2}H and ^{31}P spectra for DPPC/POPG samples containing 3 mol% SP-B_{1-25} in Fig. 3) is consistent with motions on a kHz timescale contributing to the averaging of the ^{31}P lineshapes.

Addition of SP-B_{1-25} may lead to a cubic or fluid isotropic phase via vesicle fusion

The appearance of isotropic lineshapes in the ^{31}P and ^{2}H NMR spectra upon addition of peptide is consistent with the formation of micellar, cubic, or fluid isotropic lipid

phases (37,38). To determine the relative sizes of the lipid assemblies and distinguish which lipid polymorphism results from the addition of SP-B_{1-25}, we examined the effects of peptide addition on DPPC/POPG vesicles by DLS and EM. DPPC/POPG vesicles exhibit a broad range of vesicle sizes, with an average size of ~500 nm. Addition of SP-B_{1-25} leads to the formation of larger vesicles in a concentration-dependent manner (Fig. S4). No vesicles < 150 nm are seen in the peptide-containing samples, ruling out micelle formation, and a rise in vesicles > 4000 nm is observed. The DLS instrument setup is unable to determine vesicle sizes above 10,000 nm, but a clear trend toward larger sizes is observed for samples containing higher mol% SP-B_{1-25}. Of interest, the samples containing higher peptide concentrations are visibly less opaque, ruling out the possibility that the DLS data are affected by a decrease in sensitivity due to sample turbidity. Examination of lipid assemblies by EM also indicates that the addition of SP-B_{1-25} leads to the appearance of larger interconnected or fused vesicles (Fig. S4). These observations are consistent with a cubic or fluid isotropic phase via vesicle fusion.

SP-B_{1-25} partitions at the lipid interface in lipid lamellae

By analyzing the ^{2}H NMR spectra of the lipid mixtures above their lamellar phase transition temperatures, one can monitor the effect of SP-B_{1-25} on lipid acyl chain dynamics in the fluid phase. From these effects, one can infer the partitioning depth of SP-B_{1-25} into the lipid bilayers. Lipid acyl chain order parameters were determined as previously described (25). Since our lipid samples show some degree of alignment in the magnetic field, we deconvoluted the spectra using a Tikonov regularization procedure to account for vesicle alignment. The resulting order parameter profiles for the *sn*-1 chain in mixtures of DPPC-d_{62}/POPG and DPPC/POPG-d_{31} at 44°C containing various levels of SP-B_{1-25} are graphed in Fig. 4; data for POPC-$_{31}$/POPG and POPC/POPG-d_{31} samples are presented in Fig. S5. The addition of SP-B_{1-25} results in a decrease in order parameters with increasing SP-B_{1-25} concentrations for all the lipids in the two types of mixtures. A distinct drop in the order parameters is observed upon addition of 5 mol% SP-B_{1-25}. From the order parameter profiles, it can be seen that the methylenes toward the center of the bilayers are more affected than those in the plateau region. This behavior is similar to changes observed in lipid order upon addition of antimicrobial peptides (29,39,40) and suggests that the amphipathic helix of SP-B_{1-25} partitions near the lipid headgroups.

DISCUSSION

The ability of SP-B to affect the organization and structures of lipid assemblies on the micron scale is well recognized

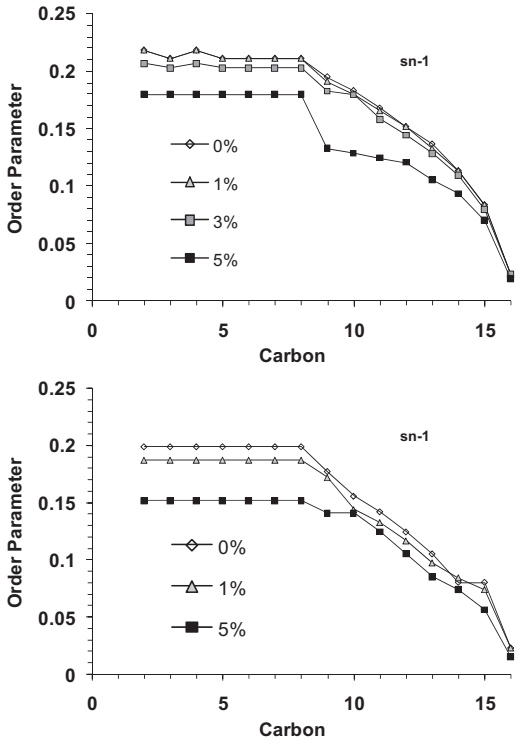

FIGURE 4 Order parameter profiles for the *sn*-1 chain of (*top*) DPPC-d_{62} in 4:1 DPPC-d_{62}/POPG and (*bottom*) POPG-d_{31} in 4:1 DPPC/POPG-d_{31} MLVs at 44°C with SP-B_{1-25} at the indicated molar percentages.

(12). These effects are particularly striking given the low physiologic concentration of SP-B, with 400–800 lipid molecules per protein monomer (9). Much of the effort toward developing synthetic replacements of PS has been focused on identifying which sequences in the highly hydrophobic SP-B are most critical for modifying lipid properties in PS. There is now a general consensus that the N- and C-termini of the protein are the most active portions of the protein (16,18,19). In this study, we focused on the effects of the N-terminal 25-residue peptide, SP-B_{1-25}, on lipid dynamics and morphology. We find that at relatively low concentrations, SP-B_{1-25} has a marked effect on lipid morphology.

SP-B_{1-25} is recognized as a surface-active and functionally important domain within SP-B, but the molecular mechanisms underlying its activity, specifically its effects on lipid organization and dynamics in bulk PS, have thus far not been fully elucidated. Previous studies focused on its surface properties via Langmuir monolayer studies of surface tension, lipid adsorption at the air-water interface, surface film stability, and film structure as a function of surface pressure (41–43). These studies are particularly germane given the role of PS in lowering surface tension and the natural air-water interface established within the lung for oxygen exchange. However, EM studies of alveolar surfaces indicate that type II pneumocytes secrete surfactant into a thin aqueous layer with an average thickness of

0.2 μm, with the bulk of the PS lipids and proteins sequestered in the aqueous subphase (44). Although SP-B has been demonstrated to promote the rapid transfer of phospholipids between the bulk aqueous phase and the air-water interface, it is not established whether SP-B itself partitions at the interface to accomplish this. For these reasons, we examined the effects of SP-B_{1-25} on lipid dynamics and organization in aqueous suspensions. Our observation by NMR of the coexistence of an isotropic phase in exchange with a lamellar phase on addition of SP-B_{1-25} to aqueous dispersions of DPPC/POPG and POPC/POPG mixtures is in good agreement with the proposed role of SP-B in aiding lipid transfer within the aqueous subphase.

Although isotropic NMR spectra for lipids are generally associated with the formation of small lipid micelles, which have correlation times shorter than the NMR timescale, other lipid polymorphisms can lead to isotropic lineshapes if the dynamics of the lipids allow individual lipid molecules to sample a broad array of orientations relative to the magnetic field on a fast enough timescale. In particular, cubic and fluid isotropic lipid phases are also consistent with isotropic NMR spectra. DLS results show that the lipid vesicle assemblies become larger rather than smaller upon peptide addition, suggesting vesicle fusion rather than micelle formation. To confirm this, we collected EM data on DPPC/POPG lipid mixtures prepared with SP-B_{1-25}. Clear fusion of the vesicles and an increase in average vesicle size is observed relative to pure lipid mixtures. However, it appears the vesicle structures are still somewhat lamellar in nature within the resolution of this technique. This suggests that the observation of an isotropic phase by NMR is due to fast exchange of the lipids between lamellae facilitated by SP-B_{1-25}. Closer inspection of the ^{2}H and ^{31}P NMR spectra support a model of SP-B_{1-25}-supported exchange of lipids between lamellae on a kHz timescale. The ^{2}H quadrupolar interaction is an order of magnitude larger than the ^{31}P chemical shift anisotropy, allowing the concurrent observation of an isotropic lineshape in the ^{31}P spectrum and a lamellar lineshape in the ^{2}H spectrum for a particular sample at temperatures where lipid exchange is intermediate between the timescales of these two interactions. This behavior is consistent with multilayer structures observed in native PS by EM and the induction of cubic phases in POPE suspensions by SP-B and SP-C (45). Additionally, EM (46), atomic force microscopy (47), and neutron reflection (48) studies have demonstrated that the film formed by PS at an air-water interface is thicker than a monolayer with an aqueous, multilayer, surface-associated surfactant reservoir. This reservoir and the secreted surfactant-containing lamellar bodies have multilayer structures that are dependent on SP-B. Our results suggest that SP-B_{1-25} may be critical for the juxtaposition of and exchange between lipid lamellae in PS.

SP-B_{1-25} may play a role not only in the organization of PS lipid assemblies, but also in lipid miscibility. DSC and ^{2}H NMR indicate that some lipid phase separation is observed upon addition of the peptide to either DPPC/POPG or POPC/POPG mixtures. Our NMR results show that SP-B_{1-25} enhances the transfer of DPPC between lipid lamellae relative to POPC and POPG at physiologic temperatures, although there is some transfer of POPC and POPG lipids as well. Alterations in ^{31}P lineshapes can be seen at lower temperatures for samples containing as little as 1 mol% SP-B_{1-25}. Motional averaging becomes more dramatic at 3 mol% SP-B_{1-25} and the extent of averaging is dependent on both the T_m of the lipid mixtures and the identity of the phospholipid headgroups. In particular, ^{2}H NMR spectra of both POPC and DPPC species exhibit isotropic lineshapes below the T_m of the POPC/POPG and DPPC/POPG mixtures, respectively. ^{31}P spectra indicate that the POPG species is also isotropic at low temperatures, but returns to a lamellar phase at lower temperatures than the PC lipids. At 5 mol% SP-B_{1-25}, the trend is even more dramatic. The ^{2}H NMR spectra for POPG-d_{31} and POPC-d_{31} are isotropic below -2°C and 6°C, respectively in POPC/POPG mixtures. In DPPC/POPG the resolution back to a lamellar lineshape is seen for POPG-d_{31} at ~34°C, but DPPC-d_{62} lineshapes remain isotropic below 40°C. This suggests that SP-B_{1-25} has an effect on lipid miscibility, particularly near the T_m of the lipid mixtures. This is especially relevant for PS, which has a T_m of ~35°C, similar to the DPPC/POPG mixture. Although physiologic levels of SP-B are much lower, at 0.1–0.2 mol%, our observation that 1 mol% SP-B_{1-25} can lead to significant averaging of the majority of the phospholipids in our mixtures suggests that even lower percentages of peptide could lead to significant transfer of lipids between lamellae. The ability of SP-B_{1-25} to nucleate a cubic or fluidic lipid phase, particularly for lipid mixtures containing DPPC, suggests a role for the N-terminus of SP-B in the packing of lipid lamellae into surfactant lamellar bodies or in stabilizing multilayer structures at the air-liquid interface. Our observation that at physiologic temperature the dynamics of DPPC lipid moiety are much more affected by SP-B_{1-25} is particularly intriguing, and suggests that SP-B may enhance the exchange of DPPC between lipid lamellae while POPG and other lipids remain within a planar lipid structure. It has been postulated DPPC may be specifically enriched at the air-water interface by PS proteins (8), and this result gives credence to that model.

Although both the N- and C-termini of SP-B have been demonstrated to have some efficacy via both in vivo and in vitro assays, the exact boundaries of the active sequences and their effects on lipid organization at the molecular level have not been fully delineated. Our finding that at relatively low concentrations SP-B_{1-25} has a marked effect on lipid morphology is in contrast to previous studies of SP-B_{8-25} (34), the C-terminus (both SP-B_{59-80} (24) and SP-B_{63-78} (49)), and a functional mimic of the C-terminus, KL_4 (25). We also note that whereas an isotropic phase has not been

observed for lipid assemblies containing SP-B_{8-25} (34), it has been observed for lipid samples containing full-length SP-B at a concentration of ~2 mol% (50,51). This indicates a specific role for the highly conserved, very hydrophobic first seven amino acids (FPIPLPY) as well as the amphiphilic helix from residues 8–22 in lipid association and remodeling. This is consistent with recent findings that the activity of a chimeric construct containing the N- and C-terminal domains of SP-B (mini-B) has superior activity upon addition of this sequence (52), and that mutations in this sequence lead to poorer reinsertion of lipids into an expanding air-water interface (19). Recent studies of surfactant systems at the air-water interface have also demonstrated that the hydrophobic N-terminus is important for stabilizing lipid nanosilos in association with POPG-enriched areas of a DPPC/POPG monolayer (53).

Molecular-dynamics simulations of SP-B_{1-25} in DPPC monolayers suggest that the most likely equilibrium conformation is with the α-helix in SP-B_{1-25} parallel to the interface (54). FTIR studies indicate that the first seven hydrophobic residues adopt a β-sheet conformation that penetrates into the interior of the lipid bilayers, with residues 8–22 forming an amphiphilic helix at the lipid bilayer interface (27). Our CD measurements are consistent with these studies and indicate that the overall structure of SP-B_{1-25} is relatively invariant with lipid composition and peptide concentration. The effects of SP-B_{1-25} on lipid acyl chain order parameters in the lamellar phase (Fig. 4) are also consistent with the peptide partitioning at the lipid interface. However, subtle differences in the effects of SP-B_{1-25} on acyl chain order within PG versus PC lipids suggest differential partitioning. Specifically, the PG acyl chains become more disordered than PC acyl chains in the lamellar phase upon addition of peptide to DPPC/POPG and POPC/POPG mixtures. Increased order in the PC acyl chains can result from either a more peripheral association of the peptide with the bilayers via electrostatic interactions (55) or the peptide partitioning more deeply into the bilayer (24,25,56). SP-B_{1-25} has a relatively high percentage of hydrophobic residues relative to other amphipathic peptides, as do all the active PS peptides, and it has a highly hydrophobic N-terminus, which would favor deeper partitioning. This observation, combined with the observed greater effects of SP-B_{1-25} on the overall organization of the PC lipids, suggests that SP-B_{1-25} may partition more deeply into PC-enriched lipid domains while remaining more surface-associated in PG-enriched lipid domains as a consequence of the differences in the charge states at the lipid interfaces (Fig. 5). This model is consistent with enzyme-linked immunosorbent assays performed using SP-B reconstituted in anionic and zwitterionic bilayers (57), which revealed that SP-B was more immunoreactive to water-soluble antibodies when it was reconstituted into anionic lipid bilayers. The deeper partitioning of SP-B_{1-25} into PC-enriched lipids would lead to negative curvature strain,

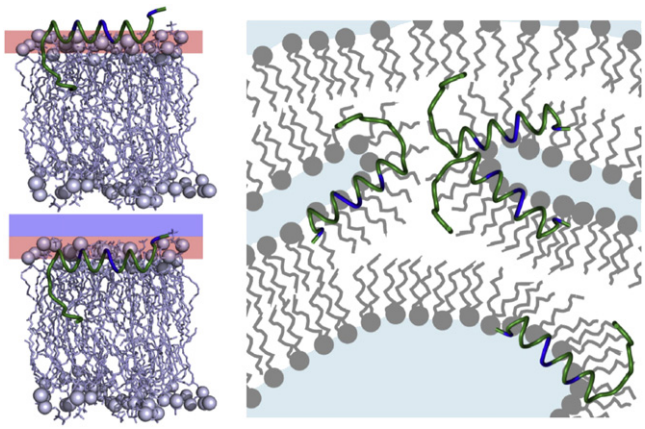

FIGURE 5 Model of SP-B_{1-25} interacting with (*top left*) anionic lipids and (*bottom left*) zwitterionic lipids, and (*right*) inducing a fluid isotropic phase in DPPC-rich regions.

which can induce lipid flipping and the formation of a cubic or fluid isotropic phase, or, at the air-water interface, enhanced adsorption of lipids to the surface monolayer from underlying lipid bilayers. The ability of SP-B_{1-25} to fuse lipid lamellae via this mechanism, particularly those enriched in DPPC, suggests a molecular mechanism for how the N-terminus of SP-B can facilitate packing of lipid lamellae into surfactant lamellar bodies or stabilize multilayer structures at the air-liquid interface. Further structural studies will assist in elucidating the mechanism by which the N-terminus modulates lipid organization in both the aqueous subphase and in association with the monolayer at the air-water interface.

CONCLUSIONS

In this study we found that SP-B_{1-25} retains a constant secondary structure when associated with lipids and causes the formation of fluid isotropic lipid phases, particularly for DPPC-containing lipid mixtures at physiologic temperatures. These findings can be compared with our previous CD and solid-state NMR studies on C-terminal SP-B peptides, where, in contrast, we found that the helical pitch of the peptide changed as the lipid milieu was altered from saturated PC to unsaturated PC, whereas there was no effect on the lipids (i.e., they remained in the lamellar mesophase). These contrasting effects suggest that the N- and C-termini of SP-B have complementary roles in trafficking of PS lipids. With the findings presented here and elsewhere, a more thorough molecular model is established that provides insights into how these small peptides modulate lipid properties that can drive the development of future SP-B mimetics. The unique interplay observed for the N- and C-termini of SP-B among lipid moieties, peptide penetration, peptide structure, and lipid polymorphisms could explain the unique properties of SP-B in the dynamic lung

environment. The synergism between these peptides is the focus of our ongoing work.

SUPPORTING MATERIAL

Additional methods, five figures, and references are available at http://www.biophysj.org/biophysj/supplemental/S0006-3495(10)00855-6.

The assistance of Dr. Alfred Chung in peptide synthesis is gratefully acknowledged. The NMR instrumentation provided by the National Science Foundation's National High Magnetic Field Laboratory is also gratefully acknowledged.

This work was supported by the National Institutes of Health (R01HL076586 to J.R.L. and R01GM077232 to G.E.F).

REFERENCES

1. Goerke, J. 1998. Pulmonary surfactant: functions and molecular composition. *Biochim. Biophys. Acta.* 1408:79–89.
2. Whitsett, J. A., and T. E. Weaver. 2002. Hydrophobic surfactant proteins in lung function and disease. *N. Engl. J. Med.* 347:2141–2148.
3. Piknova, B., V. Schram, and S. B. Hall. 2002. Pulmonary surfactant: phase behavior and function. *Curr. Opin. Struct. Biol.* 12:487–494.
4. Wright, J. R., and J. A. Clements. 1987. Metabolism and turnover of lung surfactant. *Am. Rev. Respir. Dis.* 136:426–444.
5. Veldhuizen, R., K. Nag, …, F. Possmayer. 1998. The role of lipids in pulmonary surfactant. *Biochim. Biophys. Acta.* 1408:90–108.
6. Postle, A. D., E. L. Heeley, and D. C. Wilton. 2001. A comparison of the molecular species compositions of mammalian lung surfactant phospholipids. *Comp. Biochem. Physiol. A Mol. Integr. Physiol.* 129:65–73.
7. Perkins, W. R., R. B. Dause, …, A. S. Janoff. 1996. Role of lipid polymorphism in pulmonary surfactant. *Science.* 273:330–332.
8. Veldhuizen, E. J. A., J. J. Batenburg, …, H. P. Haagsman. 2000. The role of surfactant proteins in DPPC enrichment of surface films. *Biophys. J.* 79:3164–3171.
9. Zuo, Y. Y., R. A. W. Veldhuizen, …, F. Possmayer. 2008. Current perspectives in pulmonary surfactant—inhibition, enhancement and evaluation. *Biochim. Biophys. Acta.* 1778:1947–1977.
10. Pérez-Gil, J. 2008. Structure of pulmonary surfactant membranes and films: the role of proteins and lipid-protein interactions. *Biochim. Biophys. Acta.* 1778:1676–1695.
11. Whitsett, J. A., L. M. Nogee, …, A. D. Horowitz. 1995. Human surfactant protein B: structure, function, regulation, and genetic disease. *Physiol. Rev.* 75:749–757.
12. Clark, J. C., S. E. Wert, …, J. A. Whitsett. 1995. Targeted disruption of the surfactant protein B gene disrupts surfactant homeostasis, causing respiratory failure in newborn mice. *Proc. Natl. Acad. Sci. USA.* 92:7794–7798.
13. Ballard, P. L., J. D. Merrill, …, R. A. Ballard. 2003. Surfactant protein profile of pulmonary surfactant in premature infants. *Am. J. Respir. Crit. Care Med.* 168:1123–1128.
14. Johansson, J., and T. Curstedt. 1997. Molecular structures and interactions of pulmonary surfactant components. *Eur. J. Biochem.* 244: 675–693.
15. Strayer, D. S., M. Hallman, and T. A. Merritt. 1991. Immunogenicity of surfactant. II. Porcine and bovine surfactants. *Clin. Exp. Immunol.* 83:41–46.
16. Revak, S. D., T. A. Merritt, …, C. G. Cochrane. 1991. The use of synthetic peptides in the formation of biophysically and biologically active pulmonary surfactants. *Pediatr. Res.* 29:460–465.
17. Walther, F. J., L. M. Gordon, …, A. J. Waring. 2000. Surfactant protein B and C analogues. *Mol. Genet. Metab.* 71:342–351.
18. Ryan, M. A., X. Y. Qi, …, T. E. Weaver. 2005. Mapping and analysis of the lytic and fusogenic domains of surfactant protein B. *Biochemistry.* 44:861–872.
19. Serrano, A. G., M. Ryan, …, J. Pérez-Gil. 2006. Critical structure-function determinants within the N-terminal region of pulmonary surfactant protein SP-B. *Biophys. J.* 90:238–249.
20. Sinha, S. K., T. Lacaze-Masmonteil, …, R. d'Agostino; Surfaxin Therapy Against Respiratory Distress Syndrome Collaborative Group. 2005. A multicenter, randomized, controlled trial of lucinactant versus poractant alfa among very premature infants at high risk for respiratory distress syndrome. *Pediatrics.* 115:1030–1038.
21. Seurynck, S. L., J. A. Patch, and A. E. Barron. 2005. Simple, helical peptoid analogs of lung surfactant protein B. *Chem. Biol.* 12:77–88.
22. Gupta, M., J. M. Hernández-Juviel, …, F. J. Walther. 2000. Comparison of functional efficacy of surfactant protein B analogues in lavaged rats. *Eur. Respir. J.* 16:1129–1133.
23. Waring, A. J., F. J. Walther, …, J. A. Zasadzinski. 2005. The role of charged amphipathic helices in the structure and function of surfactant protein B. *J. Pept. Res.* 66:364–374.
24. Antharam, V. C., R. S. Farver, …, J. R. Long. 2008. Interactions of the C-terminus of lung surfactant protein B with lipid bilayers are modulated by acyl chain saturation. *Biochim. Biophys. Acta.* 1778:2544–2554.
25. Antharam, V. C., D. W. Elliott, …, J. R. Long. 2009. Penetration depth of surfactant peptide KL_4 into membranes is determined by fatty acid saturation. *Biophys. J.* 96:4085–4098.
26. Gordon, L. M., S. Horvath, …, A. J. Waring. 1996. Conformation and molecular topography of the N-terminal segment of surfactant protein B in structure-promoting environments. *Protein Sci.* 5:1662–1675.
27. Gordon, L. M., K. Y. C. Lee, …, A. J. Waring. 2000. Conformational mapping of the N-terminal segment of surfactant protein B in lipid using ^{13}C-enhanced Fourier transform infrared spectroscopy. *J. Pept. Res.* 55:330–347.
28. Shanmukh, S., N. Biswas, …, R. A. Dluhy. 2005. Structure and properties of phospholipid-peptide monolayers containing monomeric SP-$B_{(1-25)}$ II. Peptide conformation by infrared spectroscopy. *Biophys. Chem.* 113:233–244.
29. Ramamoorthy, A., S. Thennarasu, …, L. Maloy. 2006. Solid-state NMR investigation of the membrane-disrupting mechanism of antimicrobial peptides MSI-78 and MSI-594 derived from magainin 2 and melittin. *Biophys. J.* 91:206–216.
30. Sternin, E., H. Schäfer, …, K. Gawrisch. 2001. Simultaneous determination of orientational and order parameter distributions from NMR spectra of partially oriented model membranes. *J. Magn. Reson.* 149:110–113.
31. Petrache, H. I., S. W. Dodd, and M. F. Brown. 2000. Area per lipid and acyl length distributions in fluid phosphatidylcholines determined by (^{2})H NMR spectroscopy. *Biophys. J.* 79:3172–3192.
32. Andrade, M. A., P. Chacón, …, F. Morán. 1993. Evaluation of secondary structure of proteins from UV circular dichroism spectra using an unsupervised learning neural network. *Protein Eng.* 6: 383–390.
33. Sáenz, A., O. Cañadas, …, C. Casals. 2006. Physical properties and surface activity of surfactant-like membranes containing the cationic and hydrophobic peptide KL_4. *FEBS J.* 273:2515–2527.
34. Russell-Schulz, B., V. Booth, and M. R. Morrow. 2009. Perturbation of DPPC/POPG bilayers by the N-terminal helix of lung surfactant protein SP-B: a ^{2}H NMR study. *Eur. Biophys. J.* 38:613–624.
35. Liu, F., R. N. A. H. Lewis, …, R. N. McElhaney. 2002. Effect of variations in the structure of a polyleucine-based α-helical transmembrane peptide on its interaction with phosphatidylcholine bilayers. *Biochemistry.* 41:9197–9207.
36. Bunow, M. R., and I. W. Levin. 1977. Raman spectra and vibrational assignments for deuterated membrane lipids. 1,2-Dipalmitoyl phosphatidylcholine-d_9 and -d_{62}. *Biochim. Biophys. Acta.* 489:191–206.

37. Epand, R. M. 1998. Lipid polymorphism and protein-lipid interactions. *Biochim. Biophys. Acta.* 1376:353–368.

38. Cullis, P. R., and B. de Kruijff. 1979. Lipid polymorphism and the functional roles of lipids in biological membranes. *Biochim. Biophys. Acta.* 559:399–420.

39. Henzler-Wildman, K. A., G. V. Martinez, …, A. Ramamoorthy. 2004. Perturbation of the hydrophobic core of lipid bilayers by the human antimicrobial peptide LL-37. *Biochemistry.* 43:8459–8469.

40. Porcelli, F., B. Buck, …, G. Veglia. 2004. Structure and orientation of pardaxin determined by NMR experiments in model membranes. *J. Biol. Chem.* 279:45815–45823.

41. Bruni, R., H. W. Taeusch, and A. J. Waring. 1991. Surfactant protein B: lipid interactions of synthetic peptides representing the amino-terminal amphipathic domain. *Proc. Natl. Acad. Sci. USA.* 88:7451–7455.

42. Longo, M. L., A. M. Bisagno, …, A. J. Waring. 1993. A function of lung surfactant protein SP-B. *Science.* 261:453–456.

43. Lee, K. Y. C., M. M. Lipp, …, A. J. Waring. 1997. Effects of lung surfactant specific protein SP-B and model SP-B peptide on lipid monolayers at the air-water interface. *Colloid Surface A.* 128:225–242.

44. Bastacky, J., C. Y. C. Lee, …, J. A. Clements. 1995. Alveolar lining layer is thin and continuous: low-temperature scanning electron microscopy of rat lung. *J. Appl. Physiol.* 79:1615–1628.

45. Chavarha, M., H. Khoojinian, …, S. B. Hall. 2010. Hydrophobic surfactant proteins induce a phosphatidylethanolamine to form cubic phases. *Biophys. J.* 98:1549–1557.

46. Bachofen, H., U. Gerber, …, S. Schürch. 2005. Structures of pulmonary surfactant films adsorbed to an air-liquid interface in vitro. *Biochim. Biophys. Acta.* 1720:59–72.

47. Diemel, R. V., M. M. E. Snel, …, J. J. Batenburg. 2002. Multilayer formation upon compression of surfactant monolayers depends on protein concentration as well as lipid composition. An atomic force microscopy study. *J. Biol. Chem.* 277:21179–21188.

48. Follows, D., F. Tiberg, …, M. Larsson. 2007. Multilayers at the surface of solutions of exogenous lung surfactant: direct observation by neutron reflection. *Biochim. Biophys. Acta.* 1768:228–235.

49. Yang, T. C., M. McDonald, …, V. Booth. 2009. The effect of a C-terminal peptide of surfactant protein B (SP-B) on oriented lipid bilayers, characterized by solid-state ^{2}H- and ^{31}P-NMR. *Biophys. J.* 96:3762–3771.

50. Morrow, M. R., J. Stewart, …, K. M. Keough. 2004. Perturbation of DPPC bilayers by high concentrations of pulmonary surfactant protein SP-B. *Eur. Biophys. J.* 33:285–290.

51. Dico, A. S., J. Hancock, …, K. M. Keough. 1997. Pulmonary surfactant protein SP-B interacts similarly with dipalmitoylphosphatidylglycerol and dipalmitoylphosphatidylcholine in phosphatidylcholine/phosphatidylglycerol mixtures. *Biochemistry.* 36:4172–4177.

52. Walther, F. J., A. J. Waring, …, R. H. Notter. 2010. Critical structural and functional roles for the N-terminal insertion sequence in surfactant protein B analogs. *PLoS ONE.* 5:e8672.

53. Frey, S. L., L. Pocivavsek, …, K. Y. Lee. 2010. Functional importance of the NH_2-terminal insertion sequence of lung surfactant protein B. *Am. J. Physiol. Lung Cell. Mol. Physiol.* 298:L335–L347.

54. Kandasamy, S. K., and R. G. Larson. 2005. Molecular dynamics study of the lung surfactant peptide SP-B_{1-25} with DPPC monolayers: insights into interactions and peptide position and orientation. *Biophys. J.* 88:1577–1592.

55. Laroche, G., E. J. Dufourc, …, J. Dufourcq. 1990. Coupled changes between lipid order and polypeptide conformation at the membrane surface. A ^{2}H NMR and Raman study of polylysine-phosphatidic acid systems. *Biochemistry.* 29:6460–6465.

56. Paré, C., M. Lafleur, …, R. N. McElhaney. 2001. Differential scanning calorimetry and (^{2})H nuclear magnetic resonance and Fourier transform infrared spectroscopy studies of the effects of transmembrane α-helical peptides on the organization of phosphatidylcholine bilayers. *Biochim. Biophys. Acta.* 1511:60–73.

57. Oviedo, J. M., C. Casals, and J. Pérez-Gil. 2001. Pulmonary surfactant protein SP-B is significantly more immunoreactive in anionic than in zwitterionic bilayers. *FEBS Lett.* 494:236–240.